Available online at www.eccomasproceedia.org
Eccomas Proceedia COMPDYN (2023) 1894-1905

ECCOMAS Proceedia

COMPDYN 2023
9th ECCOMAS Thematic Conference on
Computational Methods in Structural Dynamics and Earthquake Engineering
M. Papadrakakis, M. Fragiadakis (eds.)
Athens, Greece, 12-14 June 2023

SEISMIC RESPONSE OF DIFFERENT MASONRY BUILDING AGGREGATE CONFIGURATIONS BY A REFINED FE MODEL

Marilisa Di Benedetto[1], Fabio Di Trapani[1], Sofia Villar[1] Massimo Petracca[2], Guido Camata[3]

[1] Dipartimento di Ingegneria Strutturale, Edile e Geotecnica, Politecnico di Torino
Corso Duca degli Abruzzi 24, 10129, Turin, Italy
fabio.ditrapani, marilisa.dibenedetto@polito.it, villar.sofia.97@gmail.com

[2] ASDEA Software Technology
Via Alide Breviglieri 8, Pescara, Italy
m.petracca@asdea.net

[3] Dipartimento di Ingegneria e Geologia, Università degli studi "G. D'Annunzio" di Chieti-Pescara
Viale Pindaro 42, Pescara, Italy
g.camata@unich.it

Abstract

Unreinforced masonry (URM) aggregate buildings represent a significant portion of Italian-built heritage, especially in historical centers. These structures derive from the progressive transformation of structural units during the time, for example, because of the addition of new structural portions to existing ones. Masonry aggregates are characterized by a large number of possible configurations, including different interstorey heights, number of stories, different planar shapes and various arrangements of the masonry and structural details. Moreover, the degree of connection between the structural units is a relevant element of uncertainty conditioning the response. This paper presents a numerical study investigating the behavior of a reference-building aggregate by examining two different boundary conditions: the rigid diaphragm and the flexible diaphragm. The adopted numerical model employs a homogenized masonry approach by means of layered 2D shell elements. The models are realized with the STKO software platform for OpenSees. Nonlinear static analyses are carried out for the different case-studies highlighting the influence of the aforementioned parameters on the in-plane response of the structural units and the extent of the so-called "aggregate effect".

Keywords: Building aggregate, Aggregate effect, Homogenized masonry, OpenSees, STKO.

ISSN:2623-3347 © 2023 The Authors. Published by Eccomas Proceedia.
Peer-review under responsibility of the organizing committee of COMPDYN 2023.
doi: 10.7712/120123.10529.21369

1 INTRODUCTION

Past and recent seismic events have highlighted the vulnerability associated with unreinforced masonry building aggregates, which are typical building typologies of historical centers in Italy and in the countries of the Mediterranean area (Fig. 1). Building aggregates are formed through a process of subsequent building expansion, where new structural units are added, or connected to the existing ones, resulting in a complex structural configuration of buildings made different materials, construction methods, and restraint conditions. The structural units can share the same boundary walls, or the boundary wall can be independent. The degree of connection of the structural units is then uncertain, as well as its influence on the overall structural response under lateral loads.


a)

b)

Figure 1. Typical masonry building aggregate of Italian centers: a) Historical center of Visso b) Historical centre of Bologna.

Some recent studies have investigated the seismic behavior of masonry buildings in aggregate, and on the role of the so called "aggregate effect", namely the modification of the response of each structural unit in aggregate with respect to the individual one. Some of these studies addressed the derivation of fragility curves of real case studies [1-3] by performing numerical simulations. In most cases, the equivalent frame approach was preferred to use due to the size of the computational problem [4-5]. However, other authors provided numerical investigations on large URM compounds making use of 2D [6] and 3D [7] finite element modelling or using the discrete element method [8]. Recent experimental shake-table tests were also carried out on half-scale building aggregates [9-11] and accompanied by numerical interpretation of the damage frameworks. The aggregate effect was explicitly assessed in a recent paper by Angiolli et al. [12], in which different case studies of URM aggregates were investigated by performing nonlinear static analyses, with a 3D equivalent frame modelling approach by supposing different connection degrees and floor flexibility.

The aforementioned studies have highlighted that the role of the aggregate effect can be beneficial to the overall response if an adequate degree of connection is ensured. However, a large number of variables can affect the configuration of a URM aggregate, therefore a generalization of the problem is not possible and deserves major investigation.

Considering this framework of reference, this paper presents a numerical study aimed at the investigation of the seismic behavior of URM aggregates. A three-structural unit aggregate is defined as a reference. The structural model is realized in OpenSees [13] with the aid of the STKO software platform [14]. A refined homogenized modelling approach is used for the masonry, using 2D shell-layered finite elements. The inelastic response of the single structural units is extrapolated from the aggregate configuration as well as analyzing them as isolated. The influence of floor flexibility is also investigated. Results will show that the aggregate effect can be a beneficial impact on the seismic performance, although this mainly depends on the position of a structural unit within the building aggregate.

2 REFINED FE MODELLING OF A MASONRY BUILDING AGGREGATE

2.1 Reference case study

The reference building aggregate consists of three units, each with three stories. The central unit (Unit 2) shares the same divisor wall with the external units (Unit 1 and Unit 3). The aggregate is 11.2 m tall and measures 24 x 12.6 m in the longitudinal and transverse directions respectively. All the external walls have a thickness of 50 cm, while internal and shared walls have a thickness of 50 cm at the base, followed by a thickness of 30 cm in the rest of the stories. The floor is composed of wooden beams supporting the floor's vertical loads. The geometry of the reference case study is reported in detail in Figure 2.

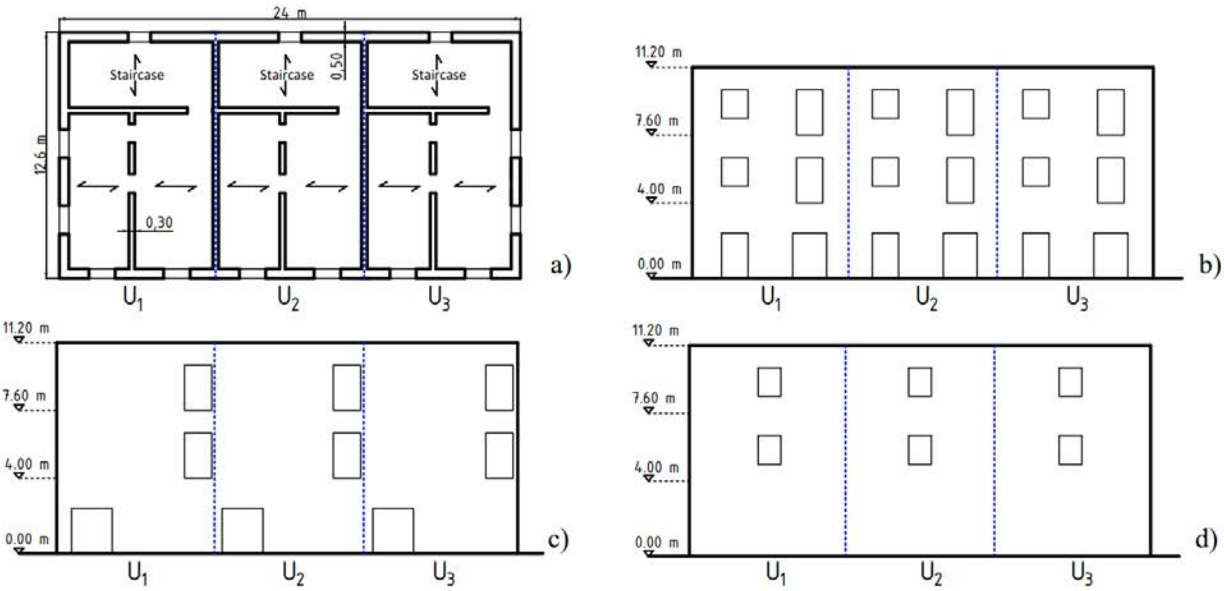

Figure 2: Reference Aggregate's geometry: a) Plan of the first storey; b) Front wall; c) Middle wall d) Back wall.

The masonry mechanical parameters are the same for the different units, and they are supposed to be those obtained from the material tests carried out at the University of Pavia [15, 16] supporting the experimental test of a full-scale masonry building structure [17, 18]. The masonry mechanical parameters are reported in Table 1.

Tensile strength f_t (MPa)	**Compressive strength f_m** (MPa)	**Elastic modulus E_m** (MPa)
0.15	6.2	1490

Table 1: Masonry mechanical properties.

The reference building aggregate was analyzed supposing the units to be fully connected or as individual structural units. For both cases, rigid floor and flexible floor conditions were investigated. The case study test configurations are summarized in Table 2.

Floor type	Unit configuration
Rigid	In aggregate Isolated
Flexible	In aggregate Isolated

Table 2: Case study test configurations for analyses.

2.2 Refined FE modelling with OpenSees/STKO

The reference building aggregate was modelled with the STKO [14] software platform for OpenSees [13]. Masonry walls were modelled as homogenized masonry with 2D layered shell elements. The *ASDConcrete3D* constitutive model was used to reproduce advanced shear and flexural damage of the walls [14, 19, 20]. The latter employs a tension-compression damage law to account for the different responses under tension and compression, where the stress tensor σ is defined according to Equation 1 [15].

$$\sigma = (1-d^{+})\bar{\sigma}^{+} + (1-d^{-})\bar{\sigma}^{-} \tag{1}$$

in which σ is the nominal stress tensor, while $\bar{\sigma}^{+}$ and $\bar{\sigma}^{-}$ are the positive and negative components of the effective stress tensors, and the indices d^{+}/d^{-} are the damage rates in tension and compression, respectively [19]. The adopted constitutive model allows the implicit/explicit (*IMPL-EX*) integration method as an option to improve the robustness of the analysis convergence [21].

Floor beams were modelled as 1D elastic elements and were connected to the masonry walls by a node-to-element interaction to which an embedded condition (*ASDEmbeddedNodeElement)* was assigned. Lintels were modelled as solid bricks and were merged with the masonry leaving in between an outline of mortar that works as a contact element.

The model was optimized by using a 2D *layered shell* for the masonry walls, which discretizes the three-dimensional nonlinear behavior into several layers in the thickness direction [22]. This allows the simplification of the model by using shell elements instead of solid elements but still benefits from the 3D response. As an element object, the *ASDShellQ4* was used. It provides a four-node quadrilateral finite element enhanced with the *AGQ6-I* formulation, which makes the element almost insensitive to geometry distortion [23]. The mesh had a dimension of 300 x 300 mm. Figure 3 illustrates an overall scheme of the reference aggregate model. The model was arranged both considering a rigid and a flexible diaphragm constraint. In the first case, the floor nodes were constrained to move as the master node (Fig. 4a). In the second case, a finite stiffness floor is modelled through an elastic 2D plate (Fig. 4b).

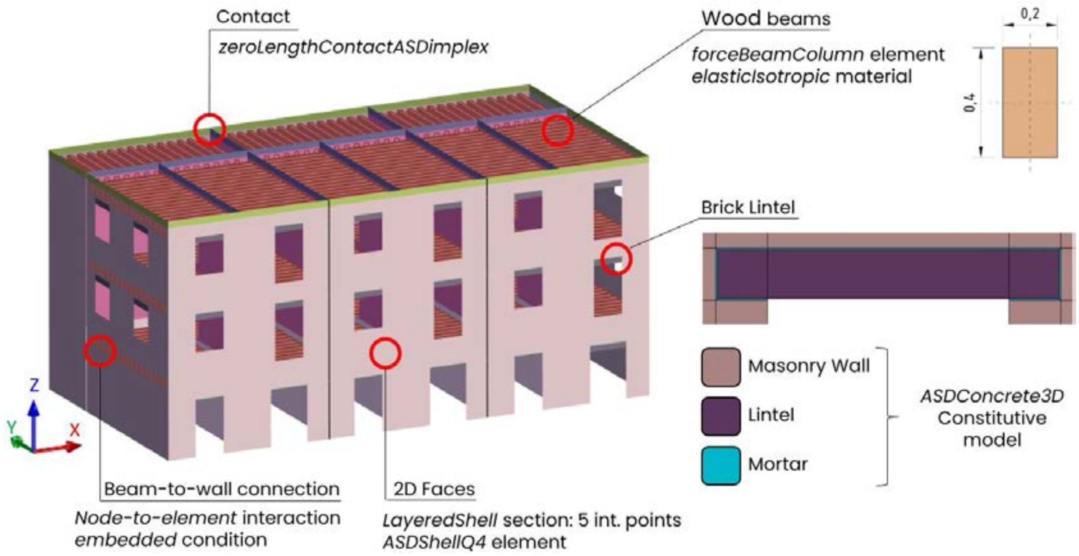

Figure 3: 2D Refined FE model of the reference building aggregate in OpenSees / STKO.

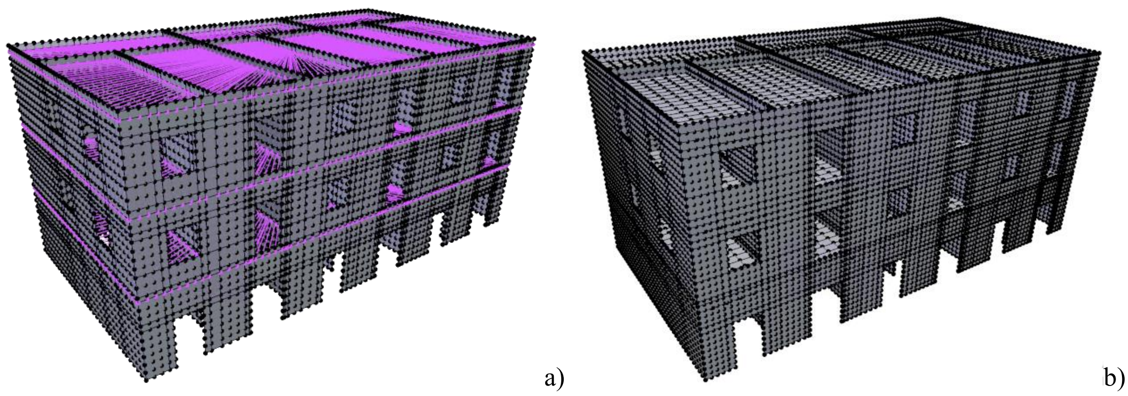

Figure 4: FE model of the reference building aggregate in OpenSees / STKO: a) with the rigid floor diaphragm; b) with the flexible floor.

Under the assumption of rigid wall-to-wall connection and a fixed base, the units were analyzed using non-linear static analysis (NSA) both in aggregate configuration and as isolated units. The NSA was performed using a lateral force distribution proportional to the fundamental mode of vibration. For this reason, the procedure involved a previous modal analysis that provided the forces' distribution. Following the same two-step procedure performed during test validation, the reference building aggregate was first loaded vertically and subsequently pushed in the longitudinal direction (X-axis). A displacement control was implemented for all NSA, with a target displacement value of 30 mm, using an Adaptive Time Step to secure convergence and the Krylov-Newton algorithm.

2.3 Preliminary validation of the model

The validation of the above-described modelling approach was carried out by reproducing the experimental response of a full-scale test on a masonry building structure tested at the University of Pavia [17, 18], which has the masonry mechanical parameters reported in Table 1. The structure is composed of two-stories and four walls. The dimensions are 6 by 4.4 m in plan and 6.4 m in elevation. The wall thickness is 250 mm. The "Door Wall" and "Window Wall" were parallel to the horizontal loading. The Door Wall was connected to the Window Wall through floor beams consisting of a series of equally spaced steel "I" profiles with a height of 140 mm designed to simulate a flexible diaphragm. The analysis was completed in two stages. First, gravity conditions were simulated by applying vertical loads through the beams. Then, a horizontal monotonic rising load is applied. The resultant displacement-reaction curves are compared to the positive experimental envelopes in Figure 5. The outcomes show that the numerical curve adequately matches the experimental results. Moreover, the numerical model was able to reproduce the crack pattern reported in the study (Fig.5b, 5c).

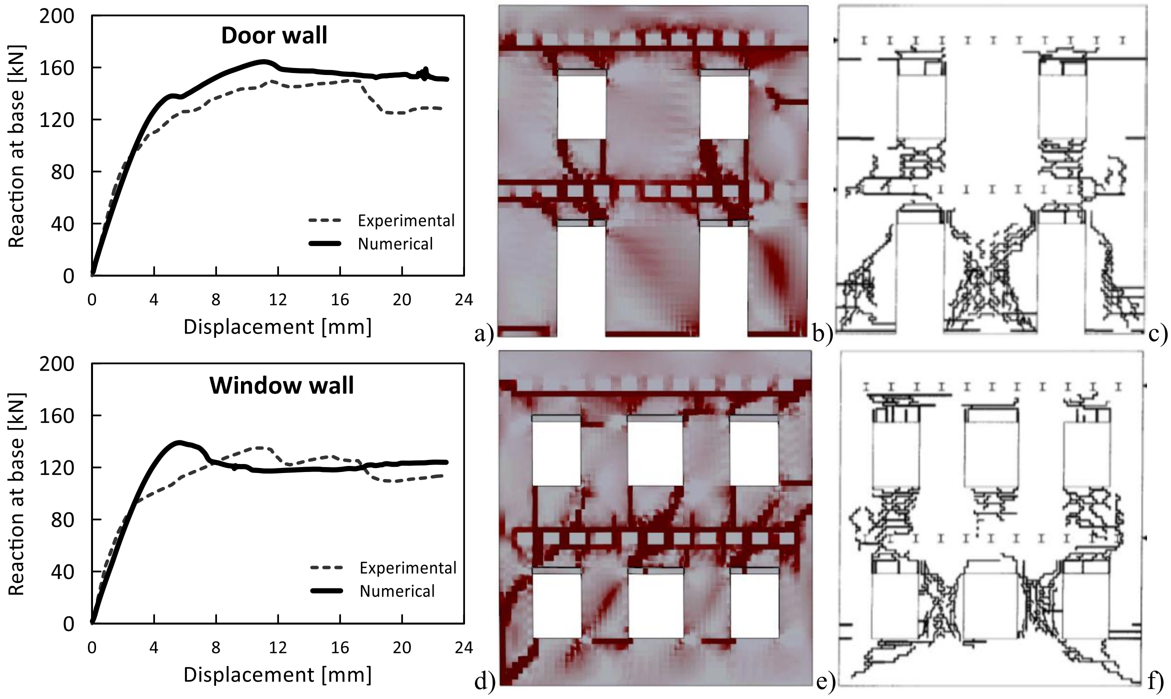

Figure 5: Numerical vs. experimental comparison: a) Pushover curves comparison b) Numerical crack pattern c) Experimental crack pattern.

3 NUMERICAL RESPONSE OF DIFFERENT AGGREGATE CONFIGURATIONS

The pushover analyses were carried out both in positive and negative longitudinal direction (X^+ axis, X^- axis). The force displacement responses were recorded for the isolated units and for the whole aggregate, deriving the corresponding response of individual units. The extrapolation of the base shear from each unit has been carried out by performing section cuts at the base of the respective walls in the X direction. Section cuts allow the extrapolation and the integration of the nodal forces as a specified section. In this way, the shear demand was isolated for each structural unit.

3.1 Rigid diaphragm configuration

The responses of the structural units in aggregate and isolated in the hypothesis of rigid diaphragm are reported in Figure 6.

The aggregate building exhibited similar behavior in both directions, with an average peak resistance of about 7000 kN (Fig. 6a). The comparison of the individual results of the units in aggregate and isolated highlights a modification of the base shear of each unit in the different configurations. Upon examining the pushover curves in Unit 1, it became apparent that pushing in the negative direction in aggregate configuration, the resistance increased by almost three times the one obtained for the isolated unit (Fig. 6b). Similarly, Unit 3 exhibited a comparable effect when pushed in the positive direction (Fig. 6d). However, when Unit 1 and Unit

3 were pushed in the opposite direction, there was no difference between the aggregate and isolated configurations (Fig. 6b, 6d). Unit 2, on the other hand, yielded nearly identical results in both directions, yet the increment of resistance with respect to the isolated configuration was less than the measured for external units (Fig. 6c). Overall, the results demonstrated that the in-aggregate configuration had a considerable beneficial effect depending on the position of the individual units and the direction of loads.

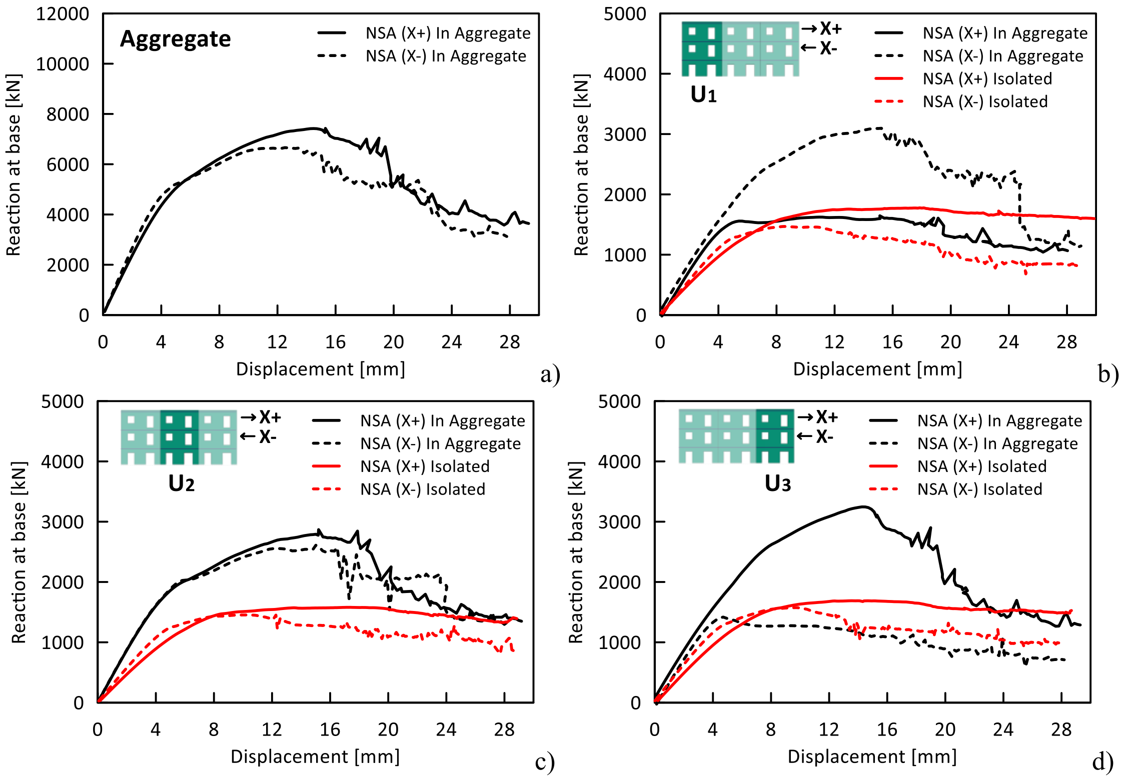

Figure 6: Numerical response comparison of building aggregate and isolated units with rigid diaphragm: (a) Overall response of building in aggregate; (b) Response of Unit 1 (c) Response of Unit 2 (d) Response of Unit 3.

Figure 7 reports the damage pattern of the building aggregate when subjected to both positive and negative pushover analysis, represented by the maximum principal force. The 3D view illustrates severe shear damage to the base masonry walls, as well as the damage sustained by the spandrels with a thinner cross-section located between the openings.

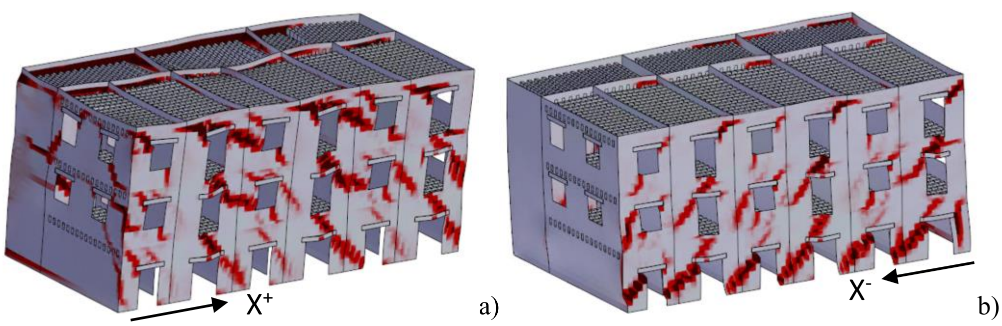

Figure 7: Crack pattern of building aggregate with rigid diaphragm: (a) Pushover X^+ (b) Pushover X^-.

The crack pattern of the building aggregate is then compared to the 3D damage of isolated units from the positive and negative pushover analysis, which is reported in Figure 8. The three units exhibited almost identical failure mechanisms, highlighting their similarity. Notably, some of the cracks that opened in the third and second floor did not extend to the base due to the increased thickness of the first-story wall (Fig. 8a). Conversely, in the negative pushover analysis, the cracks opened at the base of the building (Fig. 8b).

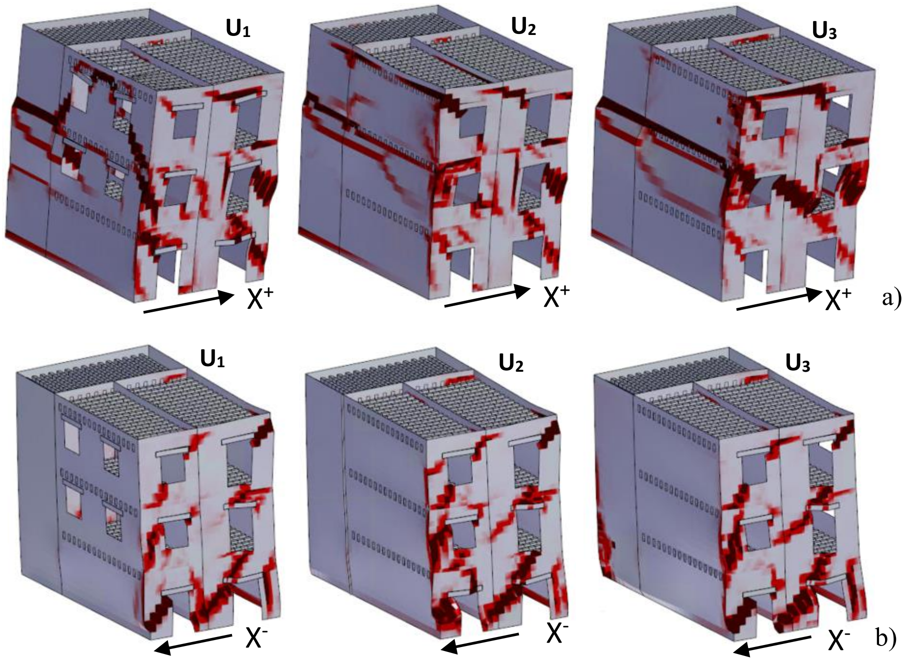

Figure 8: Numerical crack pattern of isolated units with rigid diaphragm: (a) Pushover X^+ (b) Pushover X^-.

3.2 Flexible floor configuration

The analysis procedure used for the rigid floor scenario was also employed to assess the flexible diaphragm case study test. The main outcomes are reported in Figure 9. Again, the pushover curves illustrate that the aggregate building has similar response in both positive and negative directions, reaching in average a maximum resistance of 5000 kN (Fig. 9a). As with the rigid diaphragm case, the external units (Unit 1 and Unit 3) displayed different resistance depending on the pushover direction, with an enhancement in resistance when adjacent units were present (Fig. 9b, 9c). Conversely, the central unit (Unit 2), exhibited an analogous response in both directions (Fig. 9c). Even with a flexible floor configuration, the aggregate effect was still evident but with a reduction in magnitude compared to the rigid case.

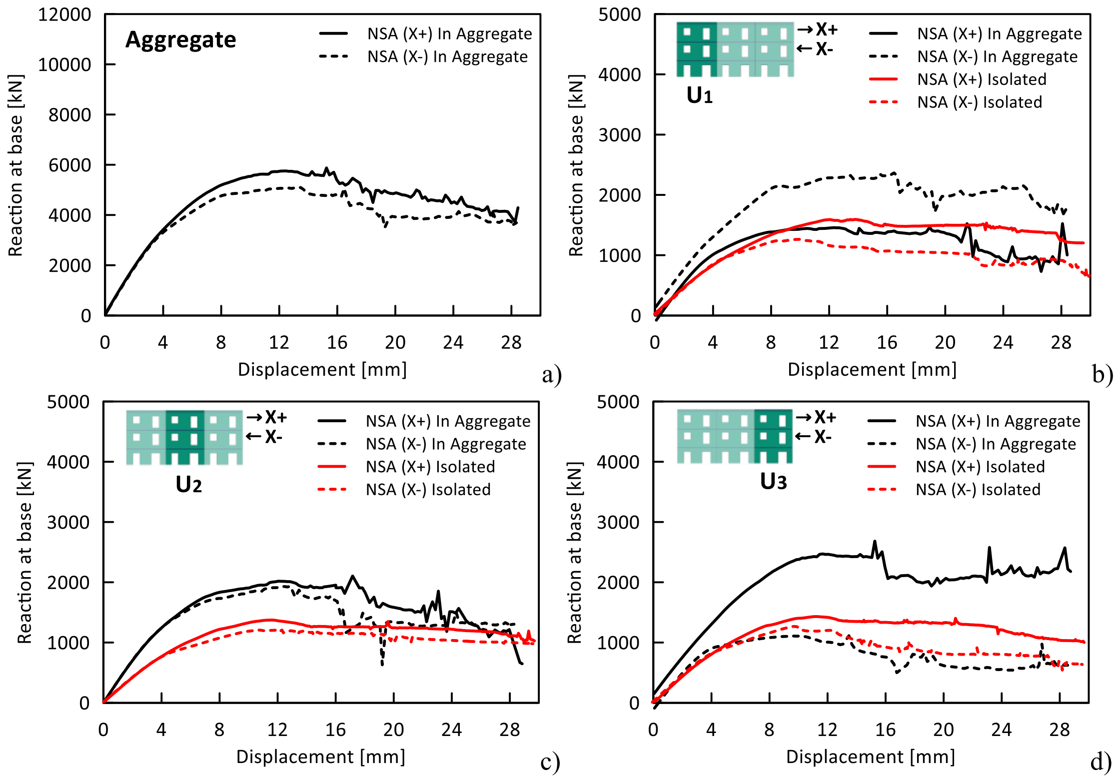

Figure 9: Numerical response comparison of building aggregate and isolated units with flexible diaphragm: (a) Global response of building aggregate (b) Response of Unit 1 (c) Response of Unit 2 (d) Response of Unit 3.

The damage patterns of the in-aggregate configuration are depicted in Figure 10 as a result of the pushover analysis in two directions. Figure 10 provides clear evidence that the shear demand moved to the front wall because of its major mass. The shear demand, and so the damage, resulted amplificated at the base of the front wall in comparison to the rigid floor case. This is the major reason for the reduction of the overall resistance.

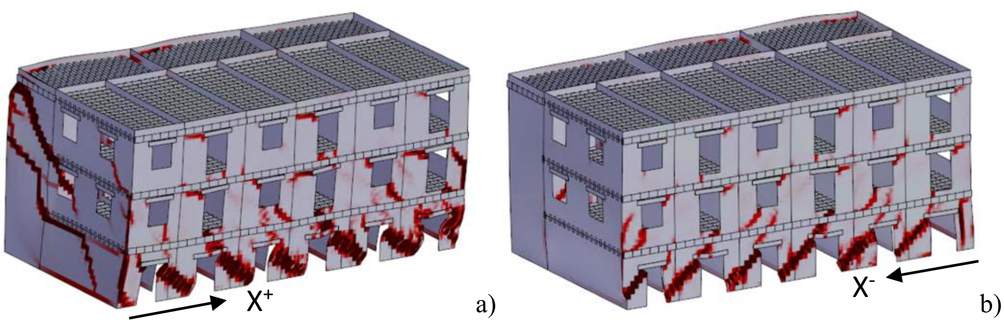

Figure 10: Numerical crack pattern of building aggregate with flexible diaphragm: (a) Pushover X^+ (b) Pushover X^-.

The crack pattern of isolated units is reported in Figure 11, where a notable depiction of damage to all unit front walls at the second-floor piers is provided.

A comparison between positive and negative pushover analyses exposes a dissimilarity in the failure mechanism of the front wall. Specifically, pushing the isolated units in the negative direction, the shear collapse occurred in the base piers instead of the second story (Fig. 11b).

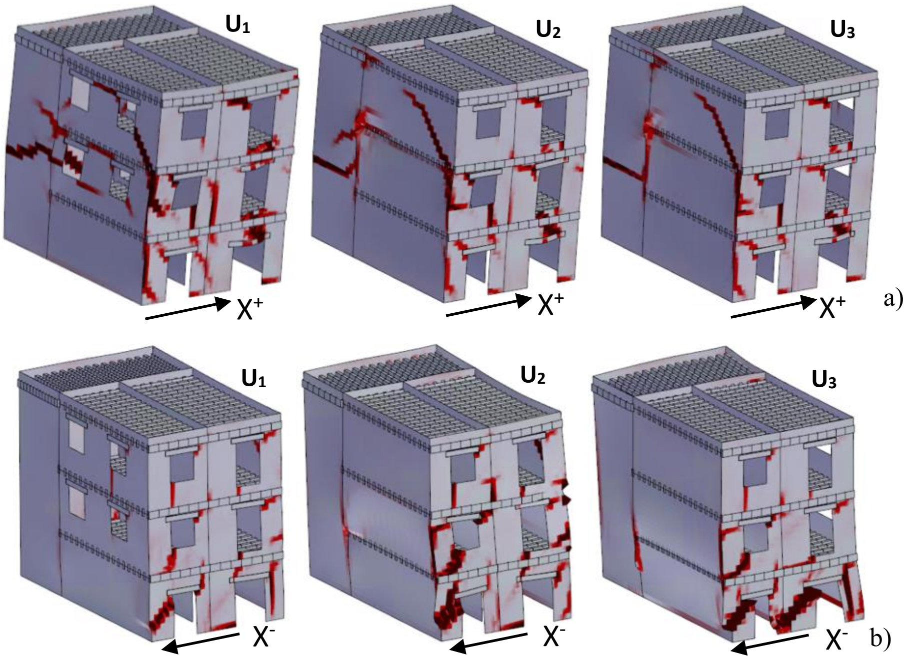

Figure 11: Numerical crack pattern of isolated units with flexible diaphragm: (a) Pushover X^+ (b) Pushover X^-.

4 CONCLUSION

Seismic response of building aggregate is complex due to the different arrangement and degree of connection of the structural units. The analysis and the assessment of these systems in the common practice is accompanied by several modelling uncertainties. In this context, the present study investigated the response of a three-unit URM aggregate to assess the potential advantages in the seismic response due to the so-called "aggregate effect".

The reference case study was modeled with the aid of the STKO software platform for OpenSees, using a homogenized masonry approach. The response of the units was recorded both in aggregate and as isolated. Also, rigid and flexible floor conditions were investigated.

The findings indicate that the overall arrangement of the units significantly influenced their performance, depending on their location and the direction of external forces. When considered together, neighboring units exhibited a group effect that enhanced their resistance, which could not be observed when analyzing each unit as isolated. This beneficial effect is still apparent even with a flexible floor configuration, although to a lesser extent compared to the rigid floor case. In conclusion, the seismic response of building aggregate can take advantage of the aggregate effect, however, more detailed studies are needed for its quantification and possible simplified modelling.

ACKNOWLEDGEMENTS

This study was supported by:

RETURN Extended Partnership and received funding from the European Union Next-GenerationEU (National Recovery and Resilience Plan – NRRP, Mission 4, Component 2, Investment 1.3 – D.D. 1243 2/8/2022, PE0000005) - WP 6 - Task 6.2.

REFERENCES

[1] R. Maio, R. Vicente, A. Formisano, H. Varum, Seismic vulnerability of building aggregates through hybrid and indirect assessment techniques. *Bulletin of Earthquake Engineering*, **13(10)**, 2995-3014, 2015.

[2] N. Chieffo, A. Formisano. Comparative Seismic Assessment Methods for Masonry Building Aggregates: A Case Study. *Front. Built Environ*, **5**,123, 2019.

[3] A. Brunelli, F. de Silva, S. Cattari, Observed and simulated urban-scale seismic damage of masonry buildings in aggregate on soft soil: The case of Visso hit by the 2016/2017 Central Italy earthquake. *International Journal of Disaster Risk Reduction*, **83**, 103391, 2022.

[4] C. Bernardini, R. Maio, S. Boschi, T. M. Ferreira, R. Vicente, A. Vignoli, The seismic performance-based assessment of a masonry building enclosed in aggregate in Faro (Portugal) by means of a new target structural unit approach. *Engineering Structures*, **191**, 386-400, 2019.

[5] M. Angiolilli, S. Lagomarsino, S. Cattari, S. Degli Abbati, Seismic fragility assessment of existing masonry buildings in aggregate. *Engineering Structures*, **247**, 113218, 2021.

[6] T. Ferrito, J. Milosevic, R. Bento, Seismic vulnerability assessment of a mixed masonry–RC building aggregate by linear and nonlinear analyses. *Bulletin of Earthquake Engineering*, **14**, 2299-2327, 2016.

[7] M. Valente, G. Milani, E. Grande, A. Formisano, Historical masonry building aggregates: advanced numerical insight for an effective seismic assessment on two-row housing compounds. *Engineering Structures,* **190,** 360–379: 2019.

[8] T. Ulrich, C. Negulescu, A. Ducellier, Using the discrete element method to assess the seismic vulnerability of aggregated masonry buildings. *Bull Earthquake Eng*, **13**, 3135–3150, 2015.

[9] I.E. Senaldi, G. Guerrini, P. Comini, F. Graziotti, A. Penna, K. Beyer, G. Magenes, Experimental seismic performance of a half-scale stone masonry building aggregate. *Bulletin of Earthquake Engineering*, **18**, 609-643, 2020.

[10] I. Tomic et al., Shake-table testing of a stone masonry building aggregate: overview of blind prediction study. *Bulletin of Earthquake Engineering*, https://doi.org/10.1007/s10518-022-01582-x, 2023.

[11] N. Bianchini, M.P. Ciocci, F. Solarino, A. Romanazzi, R. Ramirez, J. D'Anna, A. Aşıkoğlu. Influence of wall-to-floor connections and pounding on pre- and post-diction simulations of a masonry building aggregate tested on a shaking table, *Bulletin of Earthquake Engineering*, https://doi.org/10.1007/s10518-023-01641-x, 2023.

[12] M. Angiolli, S. Pinasco, S. Cattari, S. Lagomarsino, On the vulnerability features of historical masonry buildings in aggregate. *XIX ANIDIS Conference*, **44**, 2074–2081, Turin, Italy, September 2022.

[13] F. McKenna, G.L. Fenves, M.H. Scott, *Open system for earthquake engineering simulation*. University of California, Berkeley, CA, 2000.

[14] M. Petracca, F. Candeloro, G. Camata, *ASDEA Software STKO user manual*, 2017.

[15] L. Binda, G. Roberti, C. Mirabella and Abbaneo, S. Tiraboschi, Measuring masonry material Properties. *Proceeding of the U.S.-Italy Workshop on Guidelines for Seismic*

Evaluation and Rehabilitation of Unreinforced Masonry Buildings (Technical report NCEER-94-0021), Pavia, Italy, June 22-24, 1994.

[16] A. Anthoine, G. Maganotte, G. Magenes, Shear-compression testing and analysis of brick masonry walls. *Proceedings of the 10th European conference on earthquake engineering, vol 3*, Vienna, Austria, 1994.

[17] G. Magenes, G.M. Calvi, Experimental Research on Response of URM Building Systems. *Proceeding of the U.S.-Italy Workshop on Guidelines for Seismic Evaluation and Rehabilitation of Unreinforced Masonry Buildings (Technical report NCEER-94-0021)*, Pavia, Italy, June 22-24, 1994.

[18] G. Magenes, G.M. Calvi, G.R. Kingsley, Seismic Testing of a Full-Scale, Two-Story Masonry Building: Test Procedure and Measured Experimental Response. *Experimental and Numerical Investigation on a brick Masonry Building Prototype - Numerical Prediction of the Experiment, Report 3.0 - G.N.D.T*, Pavia, Italy 1995.

[19] M. Petracca, L. Pelà, R. Rossi, S. Zaghi, G. Camata, E. Spacone, E, Microscale continuous and discrete numerical models for nonlinear analysis of masonry shear walls. *Construction and Building Materials* **149**, 296-314, 2017.

[20] M.Petracca, G. Camata, E. Spacone, L. Pelà, Efficient Constitutive Model for Continuous Micro-Modeling of Masonry Structures. *International Journal of Architectural Heritage,* **17:1**, 134-146, 2023.

[21] J. Oliver, A.E. Huespe, J.C. Cante, An implicit/explicit integration scheme to increase computability of non-linear material and contact/friction problems. *Computer Methods in Applied Mechanics and Engineering*, **197**, 1865-1889, 2008.

[22] L. Xie, X. Lu, X. Lu, Y. Huang, L. Ye, Multi-Layer Shell Element for Shear Walls in OpenSees. *Computing in civil and building engineering*, 1190-1197, 2014.

[23] Chen, X. M., Cen, S., Long, Y. Q., & Yao, Z. H., Membrane elements insensitive to distortion using the quadrilateral area coordinate method. *Computers & Structures*, **82(1)**, 35-54, 2004.